ChemComm

Cite this: *Chem. Commun.*, 2011, **47**, 7656–7658

www.rsc.org/chemcomm

COMMUNICATION

Insulating diamond particles as substrate for Pd electrocatalysts†

Amy Moore,[a] Verónica Celorrio,[b] María Montes de Oca,[a] Daniela Plana,[a] Wiphada Hongthani,[a] María J. Lázaro[b] and David J. Fermín*[a]

Received 24th April 2011, Accepted 20th May 2011
DOI: 10.1039/c1cc12387d

The suitability of insulating highly crystalline diamond particles as support for Pd based electrocatalysts is explored for the first time by evaluating the electrochemical stripping of CO and oxidation of formic acid in acid solutions.

Carbon supports play a fundamental role on the efficiency of electrocatalysts in low temperature fuel cells.[1] A conventional approach in the preparation of highly dispersed metal nanostructures involves the impregnation of the metal precursor in a highly porous carbon matrix, followed by chemical reduction employing compounds such as hydrazine, borohydride, formic acid or fomaldehyde.[2] The presence of functional groups at the carbon surface can have a strong influence on the metal particle size, morphology, stability and homogeneity of the dispersion.[3] Vulcan XC-72R (Vulcan) is the most widely used carbon support in this context, due to a combination of high specific surface area and electrical conductivity.[4] On the other hand, novel materials such as carbon xerogels, nanotubes and graphene may provide new avenues for developing highly active electrocatalysts.[4,5] In this communication, we shall explore an entirely new approach, based on highly crystalline insulating diamond particles (DP) acting as supports for metal nanostructures.

Diamond is characterised by high chemical, thermal and mechanical stability and is currently being considered not only in the electrocatalysis field,[6] but also for a host of applications ranging from thermal emitters to sensing devices and biomarkers.[7] Undoped diamond is essentially an insulator with a band gap of 5.5 eV. However, hydrogen terminated surfaces are characterised by an unusual surface conductivity in contact with air or aqueous solution,[8] which is not readily observed in oxygen terminated diamond surfaces. Insulating diamond powders have been used as supports for metals such as Pd and Co in heterogeneous catalytic systems.[9] However, it would be counterintuitive to consider this material in fuel cell electrocatalysis in view of its wide band gap and complex surface chemistry. In recent years, significant work has been done to demonstrate that conducting boron doped diamond (BDD) films have unique properties as electrode supports, particularly in the context of dimensionally stable anodes.[6a,10] Recent reports have described electrocatalysts supported on BDD powders for fuel cell applications.[10,11] Here, we shall demonstrate that Pd nanostructures supported on *insulating crystalline* diamond particles can be used effectively as electrode material. Our findings not only raise fundamental questions about charge transport on wide band gap materials, but also demonstrate the possibility of employing material such as High Pressure High Temperature (HPHT) diamond powders as electrocatalyst support, a material more readily available than BDD powders.

HPHT type Ib diamond particles featuring a nominal size of 500 nm (Microdiamant AG-MSY005) were employed as the base material. HPHT diamond exhibits a significant higher degree of crystallinity and low density of sp^2 carbon impurities in comparison to particles obtained by detonation. These surface groups are of paramount importance on the electrochemical properties of diamond powders.[7c,8a] The Pd electrocatalyst supported on DP (Pd/DP) was prepared by impregnating the carbon supports with a solution of sodium hexachloropalladate(IV) tetrahydrate followed by reduction with sodium borohydride (details in the electronic supplementary information ESI). In order to compare the properties of the Pd/DP catalyst, the same procedure was followed using Vulcan as support (Pd/Vulcan). The metal loading in both catalysts was between 35 and 40%, as estimated from EDX.

Characteristic X-ray diffractograms of the DP and the Pd/DP composite are illustrated in Fig. 1a. The XRD pattern for the diamond shows peaks at $2\theta = 43.3°$, 74.7° and 91°. The Pd/DP composite showed additional peaks at $2\theta = 39.4°$, 45.6°, 67.4° and 81.3° associated with the (111), (200), (220) and (311) Pd planes, respectively. The sharp, well-defined peaks of DP indicate the highly crystalline structure of HPHT diamond. The crystallite sizes of Pd particles in the Pd/DP composite were calculated through the Scherrer equation using the (220) peak at $2\theta = 67.4°$, yielding an average crystal size of 10 nm. This region was chosen in order to avoid the influence of the signals due to the carbon substrate. Identical crystal size was estimated from the equivalent XRD peak for Pd particles supported on Vulcan (results not shown).

Fig. 1b and c illustrate a typical SEM image and the corresponding Pd distribution employing X-ray elemental mapping (recorded at 2.839 eV). The topographic features

[a] *School of Chemistry, University of Bristol, Cantocks Close, Bristol BS8 1TS, UK. E-mail: david.fermin@bristol.ac.uk; Fax: +44 1179250612; Tel: +44 117928981*
[b] *Instituto de Carboquímica (CSIC), Miguel Luesma Castán 4, 50018 Zaragoza, Spain*

† Electronic supplementary information (ESI) available: Preparation, thermogravimetric analysis and background voltammetric responses in acid solution of the Pd/DP composite. See DOI: 10.1039/c1cc12387d

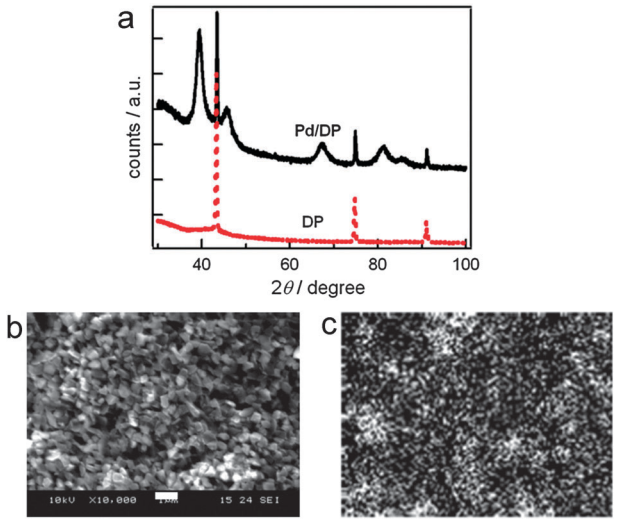

Fig. 1 XRD diffractograms of the HPHT diamond particles and the Pd/DP composite (a). The XRD data is characterised by the sharp peaks of the crystalline diamond particles and the nanoscopic Pd domains with an average particle size of 10 nm. SEM image of the Pd/DP composite (b) and Pd elemental mapping shown as white spots (c) with identical magnification. The scale bar in (b) corresponds to 1 μm. A 35–40% metal loading was obtained from EDX analysis.

of the composite are determined by the morphology of the 500 nm DP with sharp edges characteristic of HPHT materials.[8] Identical topographic features are observed in the absence of Pd particles. The elemental mapping shown in Fig. 1c reveals the areas rich in Pd as white dots scattered in a dark background corresponding to the diamond support. This image, recorded in the same scale as the SEM image in Fig. 1b, demonstrates that Pd grows as discrete particles over the entire composite.

The thermal stability of the Pd/DP and Pd/Vulcan composites, as monitored by thermogravimetric analysis, are contrasted in the supplementary information. Fig. S1† shows that the onset of Vulcan degradation shifts towards lower temperatures by 300 °C in the presence of Pd nanoparticles. On the other hand, the DP support is completely stable up to 600 °C in the presence and absence of Pd particles. A similar behaviour has been previously reported for Pt-coated BDD.[12]

Electrodes were prepared by standard drop-casting of a Nafion based ink of the Pd/DP composite on a glassy carbon electrode. The ink was prepared by mixing 2 mg of the Pd/DP composite with 50 μl of Nafion dispersion (5 wt%, Sigma-Aldrich) in 500 μl of ultrapure water (Millipore Milli-Q system). A 20 μl aliquot of this suspension was drop-casted onto a freshly polished glassy carbon electrode. The working electrode was placed in contact with the electrolyte solution in a meniscus configuration. The electrochemical cell incorporated a platinum wire as counter-electrode and a Ag/AgCl reference electrode connected by a luggin capillary. The Pd active surface area of the electrocatalyst was estimated from the CO stripping, assuming a charge per unit area of 490 μC cm^{-2}.[13] A typical cyclic voltammogram of the Pd/DP catalyst on the glassy carbon electrode in Ar-saturated 0.5 mol dm^{-3} H_2SO_4 is shown in Fig. S2† (supplementary information). Well defined responses associated with hydrogen adsorption and palladium oxide formation/reduction were obtained, providing the first set of evidence of good electronic communication through the diamond support.

The electrocatalytic properties of the Pd/DP composite towards CO oxidation, in H_2SO_4 electrolyte, were contrasted with Pd/Vulcan and the commercial Pd/C catalyst from E-Tek (20 wt% Pd supported on Vulcan). High purity CO was bubbled into the electrolyte solution for 10 min while keeping the electrode potential at −0.166 V, in order to achieve the maximum coverage of CO at the Pd centres. Subsequently, dissolved CO was purged out of the electrolyte by bubbling Ar for 20 min. Finally, two consecutive voltammograms were recorded between −0.2 and 1.0 V, at 0.02 V s^{-1}. Identical procedure was implemented for all three electrocatalysts.

The voltammetric features associated with CO stripping at Pd/DP, Pd/Vulcan and E-Tek are contrasted in Fig. 2 (left). The hydrogen adsorption region appears blocked in the initial forward scan due to adsorbed CO at the Pd surface. The key feature in the first forward scan is the CO stripping peak located at 0.68 V in the Pd/DP catalysts. The disappearance of the CO stripping peak on subsequent scans, and the reappearance of hydrogen peaks at negative potentials, indicate complete removal of CO in the first scan. A somewhat larger H absorption current was observed in the presence of the Pd/Vulcan composite, which is surprising as the Pd crystalline size domains are similar. This could be caused by the presence of large Pd domains due to agglomeration of small crystallites. However, the main feature at positive potentials of Fig. 2 (left), is associated with the potential of CO stripping, which is comparable for all three catalysts. This rather unexpected result clearly shows

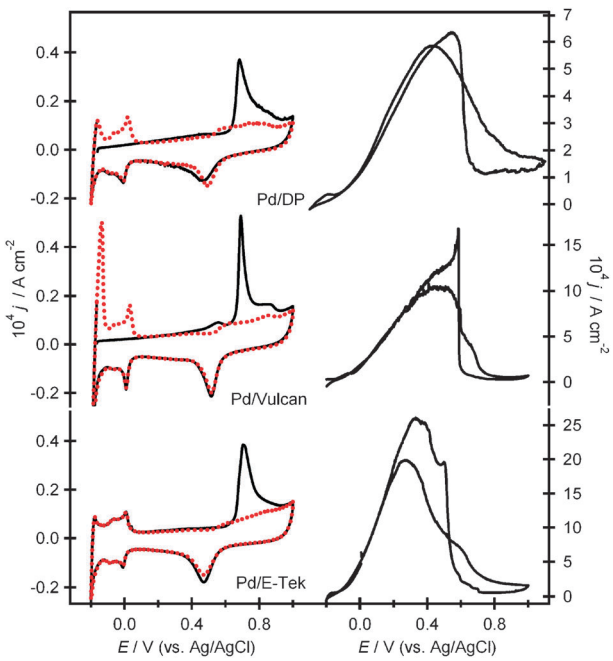

Fig. 2 CO stripping voltammograms (left) obtained for the Pd/DP, Pd/Vulcan and E-Tek electrocatalysts, at 0.02 V s^{-1}, in 0.5 mol dm^{-3} H_2SO_4. CO stripping is observed in the first scan (continuous black lines), while hydrogen adsorption/absorption responses are observed in the second scan (dashed red lines). Formic acid (2 mol dm^{-3}) oxidation was studied, under similar conditions, on the three electrocatalysts (right).

that the inherent electrocatalytic activity of Pd particles can be exploited when supported on type Ib crystalline diamond particles.

Cyclic voltammograms associated with the oxidation of formic acid (FA) at Pd/DP, Pd/Vulcan and E-Tek are also contrasted in Fig. 2 (right). These experiments provide a preliminary evaluation of the performance of the Pd/DP composite for fuel cell applications. All three catalysts show a broad peak on the forward scan and a drop in current as the Pd oxide is formed, inhibiting further FA oxidation. On reversal of the scan, once the Pd surface is recuperated, FA is once again oxidised; similar current densities are obtained on the forward and back scans indicating a high tolerance towards electrode poisoning.[14] Somewhat lower currents are obtained on Pd/DP than on the other two electrocatalysts, suggesting a smaller affinity of FA to the diamond surface as opposed to the more porous Vulcan substrate. However, this factor can be counterbalanced by the far superior stability provided by the DP. In future work, we shall investigate this reaction further, as well as the oxidation of other fuel cell relevant compounds such as methanol and ethanol.

An important aspect highlighted by these studies is the origin of the conductivity of the *insulating* DP support. It could be argued that the electrochemical responses are associated only with Pd particles in "physical contact" with the underlying GC electrode. This is very unlikely considering the homogeneous distribution of Pd in the ink and the strikingly similar responses observed on conducting carbons. Additionally, a progressive increase of the current is observed with successive layers of the ink on the GC electrode. High uncompensated resistance would arise if electron transport occurred only through discrete networks of Pd particles. Such resistance is incompatible with the voltammograms shown in Fig. 2 and Fig. S2† (supplementary information). We propose that the origin of the electronic communication is linked to partial hydrogenation of the DP during the reduction of the metal precursor anchored to the diamond support; generation of C–H bonds on exposure of diamond particles to sodium borohydride has recently been demonstrated through FTIR.[15] As shown recently, hydrogenation of diamond surfaces generates a shift of the surface dipole pushing the onset potential for surface hole accumulation to 0.1 eV *vs.* Ag/AgCl.[8a] Preliminary studies to be reported elsewhere revealed the transport properties are strongly dependent of the metal catalyst employed, as well as the type of diamond particle.

In conclusion, we have demonstrated that Pd nanostructures supported on highly crystalline, insulating diamond particles can potentially be used as electrocatalysts in fuel cells. A conventional impregnation method was used for growing Pd centres onto HPHT diamond powders, a material of tremendous chemical, thermal, mechanical and electrical stability. Despite the inherent bulk resistivity of DP, Pd centres appear interconnected to the electrode surface, possibly by hole mediated surface transport characteristic of hydrogenated diamond surfaces. We suggest that this surface conductivity in the Pd/DP composite is onset by partial hydrogenation of the diamond particle during the growth of the metal centres.

VC and MJL gratefully acknowledge CSIC and MICINN for the JAE grant and the financial support given through the Project MAT2008-06631-C03-01, respectively. DP and DJF acknowledge the financial support by the EPRSC (EP/H046305/1). WH and MMO acknowledge the support from the Royal Thai Government and the Mexican National Council for Science and Technology (CONACyT), respectively. The authors are indebted to Dr Neil A. Fox and Mr Jonathan Jones from the University of Bristol for their valuable support to this work.

Notes and references

1 (*a*) E. Antolini, *Appl. Catal., B*, 2009, **88**, 1–24; (*b*) A. L. Dicks, *J. Power Sources*, 2006, **156**, 128–141.
2 (*a*) J. B. Joo, P. Kim, W. Kim, Y. Kim and J. Yi, *J. Appl. Electrochem.*, 2009, **39**, 135–140; (*b*) J. H. Tian, F. B. Wang, Z. Q. Shan, R. J. Wang and J. Y. Zhang, *J. Appl. Electrochem.*, 2004, **34**, 461–467.
3 (*a*) F. Rodriguez-Reinoso, *Carbon*, 1998, **36**, 159–175; (*b*) E. Antolini, *J. Mater. Sci.*, 2003, **38**, 2995–3005.
4 Y. Y. Shao, J. Liu, Y. Wang and Y. H. Lin, *J. Mater. Chem.*, 2009, **19**, 46–59.
5 R. L. McCreery, *Chem. Rev.*, 2008, **108**, 2646–2687.
6 (*a*) F. Montilla, E. Morallon, I. Duo, C. Comninellis and J. L. Vazquez, *Electrochim. Acta*, 2003, **48**, 3891–3897; (*b*) J. Wang, G. M. Swain, T. Tachibana and K. Kobashi, *Electrochem. Solid-State Lett.*, 2000, **3**, 286–289; (*c*) J. Wang and G. M. Swain, *J. Electrochem. Soc.*, 2003, **150**, E24–E32; (*d*) Y. R. Zhang, S. Asahina, S. Yoshihara and T. Shirakashi, *Electrochim. Acta*, 2003, **48**, 741–747.
7 (*a*) C. E. Nebel, S. Dongchan, B. Rezek, N. Tokuda, H. Uetsuka and H. Watanabe, *J. R. Soc. Interface*, 2007, **4**, 439–461; (*b*) A. Krueger, *Adv. Mater.*, 2008, **20**, 2445–2449; (*c*) K. B. Holt, *Phys. Chem. Chem. Phys.*, 2010, **12**, 2048–2058.
8 (*a*) W. Hongthani, N. A. Fox and D. J. Fermin, *Langmuir*, 2011, **27**, 5112–5118; (*b*) F. Maier, M. Riedel, B. Mantel, J. Ristein and L. Ley, *Phys. Rev. Lett.*, 2000, **85**, 3472; (*c*) J. A. Garrido, A. Härtl, M. Dankerl, A. Reitinger, M. Eickhoff, A. Helwig, G. Müller and M. Stutzmann, *J. Am. Chem. Soc.*, 2008, **130**, 4177–4181.
9 (*a*) O. V. Turova, E. V. Starodubtseva, M. G. Vinogradov, V. I. Sokolov, N. V. Abramova, A. Y. Vul and A. E. Alexenskiy, *Catal. Commun.*, 2011, **12**, 577–579; (*b*) V. L. Kirillov, V. I. Zaikovskii and Y. A. Ryndin, *React. Kinet. Catal. Lett.*, 1998, **64**, 169–175; (*c*) K. Nakagawa, M. Kikuchi, M. Nishitani-Gamo, H. Oda, H. Ganto, K. Ogawa and T. Ando, *Energy Fuels*, 2008, **22**, 3566–3570.
10 J. Hu, X. Lu and J. S. Foord, *Electrochem. Commun.*, 2010, **12**, 676–679.
11 (*a*) N. Spataru, X. T. Zhang, T. Spataru, D. A. Tryk and A. Fujishima, *J. Electrochem. Soc.*, 2008, **155**, B264–B269; (*b*) G. R. Salazar-Banda, K. I. B. Eguiluz and L. A. Avaca, *Electrochem. Commun.*, 2007, **9**, 59–64.
12 L. Guo, V. M. Swope, B. Merzougui, L. Protsailo, M. H. Shao, Q. Yuan and G. M. Swain, *J. Electrochem. Soc.*, 2010, **157**, A19–A25.
13 A. M. El-Aziz and L. A. Kibler, *J. Electroanal. Chem.*, 2002, **534**, 107–114.
14 H. Miyake, T. Okada, G. Samjeske and M. Osawa, *Phys. Chem. Chem. Phys.*, 2008, **10**, 3662–3669.
15 L. La-Torre-Riveros, E. Abel-Tatis, A. Méndez-Torres, D. Tryk, M. Prelas and C. Cabrera, *J. Nanopart. Res.*, 2011, DOI: 10.1007/s11051-11010-10196-11058.

